



Air-sea momentum flux climatologies: A review of drag relation for parameterization choice on wind stress in the North Atlantic and the European Arctic

Iwona Wrobel-Niedzwiecka, Violetta Drozdowska, Jacek Piskozub¹

¹Institute of Oceanology, Polish Academy of Science, ul. Powstancow Warszawy 55, 81-712 Sopot, Poland
corresponding author: iwrobel@iopan.gda.pl

Key points: drag coefficient, European Arctic, North Atlantic, parameterizations

1 Abstract

2 In this paper we have chosen to check the differences between the relevant or most commonly
3 used parameterizations for drag coefficient (C_D) for the momentum transfer values, especially
4 in the North Atlantic (NA) and the European Arctic (EA). As is well known, the exact equation
5 in the North equation that describes the connection between the drag coefficient and wind
6 speed depends on the author. We studied monthly values of air-sea momentum flux resulting
7 from the choice of different drag coefficient parameterizations, adapted them to momentum
8 flux (wind stress) calculations using SAR wind fields, sea-ice masks, as well as integrating
9 procedures. We calculated monthly momentum flux averages on a $1^\circ \times 1^\circ$ degree grid and
10 derive average values for the North Atlantic and the European Arctic. We compared the
11 resulting spreads in momentum flux to global values and values in the tropics, an area of
12 prevailing low winds. We show that the choice of drag coefficient parameterization can lead
13 to significant differences in resultant momentum flux (or wind stress) values. We found that
14 the spread of results stemming from the choice of drag coefficient parameterization was 14 %
15 in the Arctic, the North Atlantic and globally, but it was higher (19 %) in the tropics. On
16 monthly time scales, the differences were larger at up to 29 % in the North Atlantic and 36 %
17 in the European Arctic (in months of low winds) and even 50 % locally (the area west of
18 Spitsbergen). When we chose the oldest parameterization (e.g. Wu, 1969 (W69)) values of
19 momentum flux were largest for all months, in compare to values from the two newest
20 parameterizations (Large and Yeager, 2004 (LY04) and Andreas, 2012 (A12)), in both
21 regions with high and low winds and C_D values were consistently higher for all wind speeds.
22 For global data not much seasonal change was noted due to the fact that the strongest winds are
23 in autumn and winter as these seasons are inverse by six months for the northern and southern
24 hemispheres. The situation was more complicated when we considered results from the North
25 Atlantic, as the seasonal variation in wind speed is clearly marked out there. With high winter
26 winds, the A12 parameterization was no longer the one that produces the smallest wind stress.
27 In this region, in summer, the highest wind stress values were produced by the NCEP/NCAR
28 reanalysis, where in C_D has a constant value. However, for low summer winds, it is the
29 lowermost outlier. As the A12 parameterization behaves so distinctly differently with low
30 winds, we showed seasonal results for the tropical ocean. The sequence of values for the
31 parameterization was similar to that of the global ocean, but with visible differences between
32 NCEP/NCAR, A12 and LY04 parameterizations. Because parameterization is supported with
33 the largest experimental data set observations of very low (or even negative) momentum flux



34 values for developed swell and low winds, our results suggest that most circulation models
35 overestimate momentum flux.

36 **1. Introduction**

37 Wind stress acts at the air-sea interface influence on wind-wave interaction, including
38 wind-driven surface waves, turbulence in upper and deep layers, drift currents, and the main
39 ocean currents (Zilitinkiewicz et al., 1978). The ocean surface mixed layer is a region where
40 kinematic forcing affects the exchange of horizontal momentum and controls transport from
41 the surface to depths (Gerbi et al., 2008, Bigdeli et al., 2017). Any attempt to properly model
42 the momentum flux from one fluid to another as the drag force per unit area at the sea surface
43 (surface shear stress, τ) must take into account other physical processes responsible for
44 generating turbulence such as boundary stress, boundary buoyancy flux, and wave breaking
45 (Rieder et al., 1994, Jones and Toba, 2001). Over the past fifty years, as the entirety of flux
46 data has increased many fold, multiple empirical formulas have been developed to express the
47 ocean surface momentum flux as a relationship between non-dimensional drag coefficient
48 (C_D), wind speed (U_{10}), and surface roughness (z_0) (Wu 1969, 1982; Bunker, 1976; Garratt,
49 1977; Large and Pond, 1981; Trenberth et al., 1989; Yelland and Taylor, 1996, Donelan et al.,
50 1997; Kukulka et al., 2007; Andreas et al., 2012). These formulas can be divided into two
51 groups. One group of theories gives the C_D at level z in terms of wind speed and possibly one
52 or more sea-state parameters (for example, Geernaert et al., 1987, Yelland and Taylor, 1996,
53 Enriquez and Friehe, 1997), while the second group provides formulas for roughness length z_0
54 in terms of atmospheric and sea-state parameters (for example, Wu, 1969, Donelan et al.,
55 1997, Andreas et al., 2012). It is well known that the drag coefficient is not a constant,
56 because surface roughness changes with sea state, and that it is an increasing function of wind
57 speed for moderate wind speeds in the marine atmospheric boundary layer (Foreman and
58 Emeis, 2010). On the other hand, many researchers have recently shown that results for the
59 drag coefficient are underestimated at moderate wind speeds and overestimated at high wind
60 speeds (Jarosz et al., 2007, Sahlée et al., 2012, Peng and Li, 2015, Brodeau et al., 2017).

61 In this paper we chose to check the differences between the relevant or most
62 commonly used parameterizations for drag coefficient (C_D) for momentum transfer values,
63 especially in the North Atlantic (NA) and the European Arctic (EA). As is widely known, the
64 exact equation that describes the connection between the drag coefficient and wind speed
65 depends on the author (Geernaert, 1990). Our intention here is not to re-invent or formulate a
66 new drag parameterization for the NA or the EA, but to revisit the existing definition of drag
67 parameterization, and, using satellite data, to investigate how existing formulas accommodate
68 the environment in the North. We concentrated on wind speed parameterizations, because
69 wind speed is a parameter that is available in every atmospheric circulation model. Therefore,
70 it is used in all air-sea flux parameterizations, and presently it is used even when sea state
71 provides a closer physical coupling to the drag coefficient (for review see Geernaert et al.,
72 1986).



73 To understand air-sea interaction, Taylor (1916) parameterized the wind's drag on the
74 sea surface using the bulk aerodynamic formula:

$$75 \quad \tau = \rho C_{Dz} U_z^2 \quad (1)$$

76 where (τ) is the drag per unit area of sea surface (also called surface stress or momentum flux),
77 ρ is air density, C_{Dz} is the non-dimensional drag coefficient appropriate for z height, and U_z is
78 the average wind speed at some reference height z above the sea. C_{Dz} is commonly
79 parameterized as a function of mean wind speed (m s^{-1}) for neutral-stability at a 10 m
80 reference height above mean sea level (Jones and Toba, 2001), which is identified as C_{DN10} or
81 C_{D10} (this permits avoiding deviation for the vertical flow from the logarithmic law):

$$82 \quad C_{DN10} = \frac{\tau}{\rho} U_{10}^2 = \left(\frac{u_*}{U_{10}}\right)^2 \quad (2)$$

83 where u_* is friction velocity. Alternatively, the neutrally stratified momentum flux can be
84 determined from the logarithmic profile, thus Eq. 1 can be express as:

$$85 \quad C_{DN10} = [\kappa/\ln(10/z_0)]^2 \quad (3)$$

86 where z_0 (m) is the aerodynamic roughness length, which is the height, above the surface to
87 define the measure of drag at which wind speed extrapolates to 0 on the logarithmic wind
88 profile (Andreas et al., 2012), and κ is von Kármán constant ($\kappa=0.4$).

89 At the same time, we can define the value of friction velocity (u_*) as having the
90 dimension of velocity, which is defined by the following equation:

$$91 \quad \tau = \rho u_*^2 \quad (4)$$

92 Comparison with bulk formula (1) leads to the equation:

$$93 \quad u_*^2 = C_{D10} U_{10}^2 \quad (5)$$

94 Some of the first studies (Wu, 1969, 1982, Garrat, 1977) focused on the relationship
95 between wind stress and sea surface roughness, as proposed by Charnock (1955), and they
96 formulated (for winds below 15 m s^{-1}) the logarithmic dependence of the stress coefficient on
97 wind velocity (measured at a certain height) and the von Kármán constant. Currently common
98 parameterizations of the drag coefficient are a linear function of 10 m wind speed (U_{10}), and
99 the parameters in the equation are determined empirically by fitting observational data to a
100 curve. The general form is expressed as (Guan and Xie, 2004):

$$101 \quad C_D 10^3 = (a + bU_{10}) \quad (6)$$

102 Wu (1969), based on data compiled from 12 laboratory studies and 30 oceanic
103 observations, formulated power-law (for breezes and light winds) and linear-law (for strong
104 winds) relationships between the wind-stress coefficient (C_y) and wind velocity (U_{10}) at a
105 certain height y at various sea states. In his study, he used roughness Reynolds numbers to



106 characterize the boundary layer flow conditions, and he assumed that the sea surface is
107 aerodynamically smooth in the range of $U_{10} < 3 \text{ m s}^{-1}$, transient at wind speed $3 \text{ m s}^{-1} < U_{10} <$
108 7 m s^{-1} , and aerodynamically rough at strong winds $U_{10} > 7 \text{ m s}^{-1}$. He also showed that the
109 wind-stress coefficient and surface roughness increase with wind speed at light winds ($U_{10} <$
110 15 m s^{-1}) and is constant at high winds ($U_{10} > 15 \text{ m s}^{-1}$) with aerodynamically rough flow.
111 Garratt (1977), who assessed the 10 m neutral drag coefficient (C_{DN10}) based on 17
112 publications, confirmed the previous relationship and simultaneously suggested a linear form
113 of this relationship for light wind. Wu (1980) proposed the linear-law formula for all wind
114 velocities and later (Wu, 1982) extended this even to hurricane wind speeds. All of the
115 preceding results rely heavily on the Monin-Obukhov similarity theory (MOST) in order to
116 eliminate the stability dependence by choosing 10 m as the standard reference height and
117 using data obtained under different experimental conditions (laboratory or field) and data
118 analysis. In 1981, Large and Pond's estimated momentum flux using the direct Reynolds flux
119 method and the dissipation method indicated the linear-law of C_D for wind speed in moderate
120 winds. Their results confirm the assumption that the neutral drag coefficient increases with
121 higher wind speed values and support the theoretical prediction that C_{DN} is independent of the
122 bulk stability parameter (z/L). Trenberth et al. (1989), who considered the uncertainty in C_D
123 from earlier experiments in which there were difficulties in calculations for low frequency
124 (less than 10 days), suggest incorporating a quantity called pseudostress (P), which assumes
125 using an effective drag coefficient and constant air density. Their results were based on data
126 from the European Centre for Medium Range Weather Forecasts (ECMWF) collected over
127 seven years. Yelland and Taylor (1996) presented results obtained from three cruises using
128 the inertial dissipation method in the Southern Ocean and indicate that using the linear-law
129 relationship between the drag coefficient and wind speed (for $U_{10} > 6 \text{ m s}^{-1}$) is better than
130 using friction velocities (u_*) with U_{10} . Fairall et al. (2003) used the COARE algorithm
131 (Coupled Ocean-Atmosphere Response Experiment) globally as a function of ambient
132 conditions. Their results with direct covariance flux measurements showed increases in C_{DN10}
133 values from 1.0×10^{-3} to 2.3×10^{-3} (or to 2.07×10^{-3} if inertial dissipation fluxes were used)
134 with increasing wind speed (from 3 m s^{-1} to 20 m s^{-1}). All of these studies show that
135 coefficients are not identical and vary with wind speed and atmospheric stability.

136 Authors of coupled circulation models preferred even simpler parameterizations. The
137 NCEP/ NCAR reanalysis (Kalnay et al., 1996) uses a constant drag coefficient of 1.3×10^{-3}
138 while, for example, the Community Climate System Model version 3 (Collins et al., 2006)
139 uses a single mathematical formula proposed by Large and Yeager (2004) for all wind speeds.
140 Their parameterizations explicitly or implicitly assume that equation (6) is exact. However,
141 Foreman and Emeis (2010) show that friction velocity is proportional to wind speed, but with
142 offset:

$$143 \quad u_* = aU_{10}^2 + b \quad (7)$$

144 Andreas et al. (2012), further referred to as A12, updated equation (8) based on available
145 datasets, friction velocity coefficient (u_*) versus neutral-stability wind speed at 10 m (U_{N10}),
146 and sea surface roughness (z_0), to find the best fit for parameters $a = 0.0583$ and $b = -0.243$.



147 They justify their choice by demonstrating that u^* vs. U_{N10} has smaller experimental
148 uncertainty than C_{DN10} , and that one expression of C_{DN10} for all wind speeds overstates and
149 overestimates results in low and high winds (**Figs. 7** and **8** in A12).

150 This led directly to a new C_D formulation with much lower values for light winds (4 -
151 9 m s^{-1}). These low values could explain why the observed momentum flux with light winds
152 and fast traveling swell can even be negative (Grachev and Fairall, 2001; Hanley and Belcher,
153 2008), and if true, this means that all previous parameterizations overestimate wind stress in
154 basins with prevailing light winds (for example, the tropics).

155 All the above studies propose different parameterizations (see **Fig. 1**) of the drag
156 coefficient and the function of wind speed, which reflects the difficulties in simultaneously
157 measuring at high sea stress (or friction velocity) and wind speed. The purpose of this study
158 is to show how the choice of C_D parameterization influences the value of the momentum flux
159 from the atmosphere to the ocean with observations based on wind fields in different parts of
160 the ocean, but especially in the NA and the EA seas.

161 **2. Materials and Methods**

162 We calculated monthly and annual mean momentum fluxes using a set of software
163 processing tools called FluxEngine (Shutler et al., 2016), which was created as part of the
164 OceanFlux Greenhouse Gases project funded by the European Space Agency (ESA). Since
165 the toolbox, for now, is designed to calculate only air-sea gas fluxes but it does contain the
166 necessary datasets for other fluxes, we made minor changes in the source code by adding
167 parameterizations for the air-sea drag relationship. For the calculations, we used Earth
168 Observation (EO) wind speed data at 10 m above sea level for 1992-2010 and sea roughness
169 (σ_0 – altimeter backscatter signal in the Ku band) from the GlobWave project
170 (<http://globwave.ifremer.fr/>). GlobWave produced a 20-year time series of global coverage
171 multi-sensor cross-calibrated wave and wind data, which are publicly available at the
172 Ifremer/CERSAT cloud. Satellite scatterometer derived wind fields are at present believed to
173 be at least equally as good as wind products from reanalyses (see, for example, Dukhovskoy
174 et al. 2017) for the area of our interest in the present study. The scatterometer derived wind
175 values are calibrated to the equivalent neutral-stability wind at a reference height of 10 m
176 above the sea surface, and, therefore, are fit for use with the neutral-stability drag coefficient
177 (Chelton and Freilich, 2005). Wave data were collected from six altimeter missions (like
178 Topex/POSEIDON, Jason-1/22, CryoSAT, etc.) and from ESA Synthetic Aperture Radar
179 (SAR) missions (ERS-1/2 and ENVISAT). All data came in netCDF-4 format. The output
180 data is a compilation file that contains data layers, and process indicator layers. The data
181 layers within each output file include statistics of the input datasets (e.g., variance of wind
182 speed, percentage of ice cover), while the process indicator layers include fixed masks as land,
183 open ocean, coastal classification, and ice.

184 All analyses using the global data contained in the FluxEngine software produced a
185 gridded ($1^\circ \times 1^\circ$) product. The NA was defined as all sea areas in the Atlantic sector north of
186 30° N , and the EA subset was those sea areas north of 64° N (**Fig. 6**). We also defined the



187 subset of the EA east of Svalbard (“West Svalbard” between 76° and 80° N and 10° to 16° E),
 188 because it is a region that is studied intensively by multiple, annual oceanographic ship
 189 deployments (including that of the R/V Oceania, the ship of the institution the authors are
 190 affiliated with). FluxEngine treats areas with sea-ice presence in a way that is compatible with
 191 Lüpkes et al. (2012) multiplying the water drag coefficient by the ice-free fraction of each
 192 grid element. We also define “tropical ocean” as all areas within the Tropics (23° S to 23° N,
 193 not show) in order to test the hypothesis that the new A12 parameterization will produce
 194 significantly lower wind stress values in the region.

195 In this study, we calculated air-sea momentum flux average values using seven
 196 different drag coefficient parameterizations (C_D). All of them are generated from the vertical
 197 wind profile, but they differ in the formulas used.

$$198 \quad 10^3 \cdot C_{D10} = 0.5U_{10}^{0.5} \quad \text{for } 1 \text{ m s}^{-1} < U_{10} < 15 \text{ m s}^{-1} \quad (8)$$

199 (Wu, 1969)

$$200 \quad 10^3 \cdot C_{DN10} = 0.75 + 0.067U_{10} \quad \text{for } 4 \text{ m s}^{-1} < U < 21 \text{ m s}^{-1} \quad (9)$$

201 (Garratt, 1977)

$$202 \quad 10^3 \cdot C_{D10} = (0.8 + 0.065U_{10}) \quad \text{for } U_{10} > 1 \text{ m s}^{-1} \quad (10)$$

203 (Wu, 1982)

$$204 \quad 10^3 \cdot C_{DN10} = 0.29 + \frac{3.1}{U_{10N}} + \frac{7.7}{U_{10N}^2} \quad \text{for } 3 \text{ m s}^{-1} < U_{10N} < 6 \text{ m s}^{-1} \quad (11)$$

$$205 \quad 10^3 \cdot C_{DN10} = 0.60 + 0.070U_{10N} \quad \text{for } 6 \text{ m s}^{-1} < U_{10N} < 26 \text{ m s}^{-1}$$

206 (Yelland and Taylor, 1996)

$$207 \quad 10^3 \cdot C_D = 1.3 \quad \text{everywhere} \quad (12)$$

208 (NCEP/NCAR)

$$209 \quad 10^3 \cdot C_{DN10} = \frac{2.7}{U_{10N}} + 0.142 + 0.076U_{10N} \quad \text{everywhere} \quad (13)$$

210 (Large and Yeager, 2004)

$$211 \quad C_{DN10} = \frac{u^*}{U_{10N}} = a^2 \left(1 + \frac{b}{a} U_{10N}^2\right) \quad \text{everywhere} \quad (14)$$

212 where $a = 0.0583$, $b = -0.243$ (Andreas et al., 2012)

213 where C_{DN10} is the expression of neutral-stability (10-m drag coefficient), C_{D10} is the drag
 214 coefficient dependent on surface roughness, U_{10} is the mean wind speed measured at 10 m
 215 above the mean sea surface, U_{10N} is the 10-m, neutral-stability wind speed.

216 3. Results and Discussion

217 Using FluxEngine software, we produced monthly gridded global air-sea momentum
 218 fluxes data. We calculated average momentum flux values separately for each month for the
 219 global ocean, the NA Ocean, and its subsets: the Arctic sector of the NA and the West



220 Spitsbergen area (WS). Some of the parameterizations used were limited to a restricted wind
221 speed domain. We used them for all the global wind speed data to avoid data gaps for winds
222 that were too high or too low for a given parameterization (**Fig. 1**). However, circulation
223 models have the very same constraint and, therefore, the procedure we used emulated using
224 the parameterization in oceanographic and climate modeling.

225 Since wind velocity was used to estimate C_D , **Fig. 1** shows a wide range of empirical
226 formulas and **Fig. 6** shows annual mean wind speed U_{10} (m s^{-1}) in the NA and the EA. The
227 differences between the oldest (eq. 8 - 10) and the newer (eq. 11, 13, 14) parameterizations
228 are distinct (**Fig. 1**). The C_D values from the oldest parameterizations increased linearly with
229 wind speed since the results from newer ones are sinusoidal indicating decreases for winds in
230 the range of 0 - 10 m s^{-1} , after which they began increase. Under weak winds ($< 10 \text{ m s}^{-1}$), the
231 drag coefficient values were significantly lower than under stronger winds ($> 10 \text{ m s}^{-1}$), with
232 greater differences among all used parameterizations. At a wind value of about 15 m s^{-1} , the
233 results from eq. 9, 10, and 14 overlapped providing the same values for the drag coefficient
234 parameterizations. The annual mean wind speed in the NA is 10 m s^{-1} , and in the EA it is 8.5
235 m s^{-1} (**Fig. 6**).

236 **Figure 2** presents maps of the mean boreal winter DJF and summer JJA momentum
237 fluxes for the chosen C_D parameterizations (Wu, 1969 and A12 – the ones with the largest and
238 smallest C_D values). The supplementary materials contain complete maps of annual and
239 seasonal means for all the parameterizations. The zones of the strongest winds are in the
240 extra-tropics in the winter hemisphere (southern for JJA and northern for DJF). The older Wu
241 (1969) parameterization produces higher wind stress values than A12 in both regions with
242 high and low winds and C_D values are consistently higher for all wind speeds except the
243 lowest ones (which, after multiplying by U^2 , produced negligible differences in wind stress
244 for the lowest winds). The average monthly values for each of the studied areas are shown in
245 **Fig. 3**. Generally, this illustrates that the newer the drag coefficient parameterization is, the
246 smaller the calculated momentum flux is. For global data (**Fig. 3a**), not much seasonal change
247 is noted, because the strongest winds are in fall and winter, but these seasons are the opposite
248 in the northern and southern hemispheres. The parameterization with the largest momentum
249 flux values for all months is that of Wu (1969), the oldest one, while the two
250 parameterizations with the lowest values are the newest ones (Large and Yeager, 2004 and
251 A12). For the NA (**Fig. 3b**), with is much more pronounced seasonal wind changes, the
252 situation is more complicated. With high winter winds, the A12 parameterization is no longer
253 the one that produces the smallest wind stress (it is actually in the middle of the seven).
254 However, for low summer winds, it is the lowermost outlier. Actually, in summer, the
255 constant C_D value used by the NCEP/NCAR reanalysis produces the highest wind stress
256 values in the Na. The situation is similar for the EA (a subset of the NA), the wind stress
257 values of which are shown in **Fig. 3c**, and for the WS area (not show). In the Arctic summer,
258 A12 produces the least wind stresses, while all the other parameterizations look very similar
259 qualitatively (even more so in the Arctic than in the whole NA). Because the A12
260 parameterization behaves so distinctly differently with low winds, we also show seasonal
261 results for the tropical ocean (**Fig. 3d**). The seasonal changes are subdued for the whole



262 tropical ocean with the slight domination of the Southern Hemisphere (the strongest winds are
263 during the boreal summer) with generally lower momentum transfer values (monthly averages
264 in the range of 0.2 to 0.3 N m⁻² compared to 0.2 to 0.4 N m⁻² for the NA and 0.2 to 0.5 N m⁻²
265 for the Arctic). The sequence of values for the parameterization is similar to that of the global
266 ocean, but there are differences. Here the NCEP/NCAR constant parameterization is the
267 second highest (instead of Wu, 1982 for the global ocean) while, unlike in the case of the
268 global ocean, A12 produces visibly lower values than does the Large and Yeager (2004)
269 parameterization.

270 We compared directly the results of the two parameterizations for the drag air-sea
271 relation that uses different dependencies (**Fig. 4**). For this estimation we chose the two most-
272 recent parameterizations (eq. 13 and 14) that showed the lowest values and change seasonally
273 depending on the area used. This comparison showed that the A12 parameterization
274 demonstrates almost zero sea surface drag for winds in the range of 3 - 5 m s⁻¹, which is
275 compensated for by a certain surplus value for strong winds. As a result, these months with
276 weak winds have significantly lower momentum flux values. This could be at statistical effect
277 of weak wind ocean areas having stable winds with waves traveling in the same direction as
278 the wind at similar speeds. The small drag coefficient values facilitate what Grachev and
279 Fairall (2001) describe as the transfer of momentum from the ocean to the atmosphere at wind
280 speeds of 2 - 4 m s⁻¹, which correspond to the negative drag coefficient value. Such events
281 require specific meteorologist conditions, but this strongly suggests that the average C_D value
282 for similar wind speeds could be close to zero.

283 **Table 1** and **Fig. 5** present the average air-sea momentum flux values (in N m⁻²) for all
284 the regions studied and all the parameterizations. All the values are also presented as
285 percentages of A12, which produced the lowest values for each region. A surprising result is
286 the proportionality of all the parameterizations for the global, the NA, and the Arctic regions
287 on annual scales (**Fig. 3** shows that this is not true on monthly scales). The spread of the
288 momentum flux results is 14 % in all three regions, and even flux values themselves are larger
289 in the NA than globally and larger in the Arctic than in the whole of the NA basin. The
290 smaller WS region, with winds that are, on average, weaker than those of the whole Arctic
291 (but stronger than those of the whole NA), had slightly different ratios of the resultant fluxes.
292 For the tropical ocean, which is included for comparison because of its weaker winds, the
293 spread in momentum flux values on an annual scale is 19 %. The spreads are even larger on
294 monthly scales (not shown). The difference between A12 and Wu (1969) and NCEP/NCAR
295 (the two parameterizations producing the largest fluxes on monthly scales) are 27 % and 29 %
296 for the NA (in July), 31 % and 36 % for the Arctic (in June), 42 % and 51 % for the WS
297 region (in July) and 23 % and 22 % for the tropical ocean (in April), respectively. Seasonality
298 in the tropics is weak, therefore, the smallest monthly difference of 16 % (July) is larger than
299 the difference for the global data in any month (the global differences between the
300 parameterizations have practically no seasonality). On the other hand, the smallest monthly
301 differences between the parameterizations in the NA, the Arctic, and the WS regions are all
302 7 %, in the month of the strongest winds (January).



303 Because the value of momentum flux is important for ocean circulation, its correct
304 calculation in coupled models is very important, especially in the Arctic, where cold halocline
305 stratification depends on the amount of mixing (Fer, 2009). We show that with the
306 parameterization used in modelling, such as the NCEP/NCAR constant parameterization and
307 Large and Yeager (2004), production stress results differ by about 5 %, on average (both in
308 the Arctic and globally), and the whole range of parameterizations leads to results that differ,
309 on average, by 14 % (more in low wind areas) and much more on monthly scales. One aspect
310 that needs more research is the fact that the newest parameterization, A12, produces less
311 momentum flux than all the previous ones, especially in lower winds (which, by the way,
312 continues the trend of decreasing values throughout the history of the formulas discussed).
313 The A12 parameterization is based on the largest set of measurements of friction velocity as a
314 function of wind speed and utilizes the recently discovered fact that b in equation (8) is not
315 negligible. It also fits the observations that developed swell at low wind velocity has celerity
316 which leads to zero or even negative momentum transfer (Grachev and Fairall, 2001).
317 Therefore the significantly lower A12 results for the tropical ocean (the trade wind region)
318 and months of low winds elsewhere could mean that most momentum transfer calculations are
319 overestimated. This matter needs further study, preferably with new empirical datasets.

320 **4. Conclusions**

321 We show that the choice of drag coefficient parameterization can lead to significant
322 differences in resultant momentum flux (or wind stress) values. The differences between the
323 highest and lowest parameterizations are 14 % in the Arctic, the NA, and globally, and they
324 are higher in low winds areas. The parameterizations generally have a decreasing trend in the
325 resultant momentum flux values, with the most recent (Andreas et al., 2012) producing the
326 lowest wind stress values, especially at low winds, resulting in almost 20 % differences in the
327 tropics. The differences can be much larger on monthly scales, up to 29 % in the NA and 36 %
328 in the EA (in months of low winds) and even 50 % locally in the area west of Spitsbergen. For
329 months with the highest winds, the differences are smaller (about 7 % everywhere), but
330 because the flux values are largest with high winds this discrepancy is also important for air-
331 sea momentum flux values. Since momentum flux is an important parameter in ocean
332 circulation modeling, we believe more research is needed, and the parameterizations used in
333 the models possibly need upgrading.

334 **Acknowledgements**

335
336 We would like to express our gratitude to Ed Andreas for inspiring us. His untimely departure
337 is an irreplaceable loss to the air-sea exchange community. We would also like to thank the
338 entire OceanFlux team. This publication was financed with funds from Leading National
339 Research Centre (KNOW) received by the Centre for Polar Studies for the period 2014–2018
340 and from OceanFlux Greenhouse Gases Evolution, a project funded by the European Space
341 Agency, ESRIN Contract No. 4000112091/14/I-LG.

342
343

344 **References**

- 345 Andreas, E. L., Mahrt, L., and Vickers, D.: A new drag relation for aerodynamically rough
346 flow over the Ocean, *J. Atmos. Sci.*, **69**(8), 2520-2539, doi:10.1175/JAS-D-11-0312.1,
347 2012.
- 348 Bigdeli, A., Loose, B., Nguyen, A.T., and Cole, S. T.: Numerical investigation of the Arctic
349 ice-ocean boundary layer and implications for air-sea gas fluxes, *Oce. Sci.*, **13**, 61-75,
350 doi:10.5194/os-13-61-2017, 2017.
- 351 Brodeau, L., Barnier, B., Gulev, S. K., and Woods, C.: Climatologically significant effects of
352 some approximations in the bulk parameterizations of turbulent air-sea fluxes, *J. Phys.*
353 *Oceanogr.*, **47**(1), 5-28, doi:10.1175/JPO-D-16-0169.1, 2017.
- 354 Bunker, A. F.: Computations of surface energy flux and annual air-sea interaction cycles of
355 the North Atlantic Ocean, *Mon. Weather Rev.*, **104**(9), 1122-1140, doi:10.1175/1520-
356 0493(1976)104<1122LCOSEFA>2.0.CO;2, 1976.
- 357 Charnock, H.: Wind stress on a water surface, *Quart. J. Roy. Meteor. Soc.*, **81**, 639-640,
358 doi:10.1002/qj.49708135027 551.554:551.465, 1955.
- 359 Chelton, D. B., and Freilich, M. H.: Scatterometer-Based Assessment of 10-m Wind Analyses
360 from the Operational ECMWF and NCEP Numerical Weather Prediction Models, *MWR*,
361 *Mon. Weather Rev.*, **133**, 409-429, 2005.
- 362 Collins, W. D., Bitz, C. M., Blackmon, M. L., Bonan, G. B., Bretherton, S. C., Carton, A. J.,
363 Chang, P., Doney, S. C., Hack, J. J., Henderson, T. B., Kiehl, J. T., Large, W. G.,
364 McKenna, D. S., Santer, B. D., and Smith, R. D.: The Community Climate System Model
365 version 3 (CCSM3), *J. Climate*, **19**(11), 2122–2143, doi:10.1175/JCLI3761.1, 2006.
- 366 Donelan, M. A., Drennan, W. M., and Katsaros, K. B.: The air-sea momentum flux in
367 conditions of wind sea and swell, *J. Phys. Oceanogr.*, **27**(10), 2087-2099,
368 doi:10.1175/1520-0485(1997)027<2087:TASMFI>2.0.CO;2, 1997.
- 369 Dukhovskoy, D. S., Bourassa, M. A., Peterson, G. N., and Steffen, J.: Comparison of the
370 surface vector winds from atmospheric reanalysis and scatterometer-based wind products
371 over the Nordic Seas and the northern North Atlantic and their application for ocean
372 modeling, *J. Geophys. Res.: Oceans*, **122**, 1943-1973, doi:10.1002/2016JC012453, 2017.
- 373 Enriquez, A. G., and Friehe, C. A.: Bulk parameterization of momentum, heat, and moisture
374 fluxes over a coastal upwelling area, *J. Geophys. Res.: Oceans*, **102**(C3), 5781-5798,
375 doi:10.1029/96JC02952, 1997.
- 376 Fairall, C. W., Bradley, E. F., Hare, J. E., Grachev, A. A., and Edson, J. B.: Bulk
377 parameterization of air-sea fluxes: updates and verification for the COARE algorithm, *J.*
378 *Climate*, **16**(4), 571-591, doi:10.1175/1520-0442(2003)016<0571:BPOASF>2.0.CO;2,
379 2003.
- 380 Fer, I.: Weak vertical diffusion allows maintenance of cold halocline in the central Arctic,
381 *Atmos. and Oce. Sci. Lett.*, **2**(3), 148-152, 2009.
- 382 Foreman, R. J., and Emeis, S.: Revisiting the definition of the drag coefficient in the marine
383 atmospheric boundary layer, *J. Phys. Oceanogr.*, **40**, doi:10.1175/2010JPO4420.1, 2010.
- 384 Garratt, J. R.: Review of drag coefficients over oceans and continents. *Mon. Weather Rev.*,
385 **105** (7), 915-929, doi:10.1175/1520-0493(1977)105<0915:RODCOO>2.0.CO;2, 1977.



- 386 Geernaert, G. L., Katsoros, K. B., and Richter, K.: Variation of the drag coefficient and its
387 dependence on sea state, *J. Geophys. Res.*, 91(C6), 7667-7679,
388 doi:10.1029/JC091iC06p07667, 1986.
- 389 Geernaert, G. L., Larsen, S. E. , and Hansen, F.: Measurements of the wind stress, heat flux,
390 and turbulence intensity during storm conditions over the North Sea, *J. Geophys. Res.:*
391 *Oceans*, 92(C13), 13127-13139, doi:10.1029/JC092iC12p13127, 1987.
- 392 Geernaert, G. L.: Bulk parameterizations for the wind stress and heat flux. *Surface Waves and*
393 *Fluxes*, Vol. I, G. L., Geernaert and W. L., Plant, Eds. Kluwer, 91-172, 1990.
- 394 Gerbi, G. P., Trowbridge, J. H., Edson, J. B., Plueddemann, A. J., Terray, E. A., and
395 Fredericks, J. J.: Measurements of momentum and heat transfer across the air-sea interface.
396 *J. Phys. Oceanogr.*, 38(5), 1054-1072. doi:10.1175/2007JPO3739.1, 2008.
- 397 Grachev, A. A., and Fairall, C. W.: Upward Momentum Transfer in the Marine Boundary
398 Layer, *J. Phys. Oceanogr.*, 31(7), 1698-1711, doi.org/10.1175/1520-
399 0485(2001)031<1698:UMTITM>2.0.CO;2, 2001.
- 400 Guan, C., and Xie, L.: On the linear parameterization of drag coefficient over sea surface, *J.*
401 *Phys. Oceanogr.*, 34(12), 2847-2851, <https://doi.org/10.1175/JPO2664.1>, 2004.
- 402 Hanley, K. E., and Belcher, S. E.: Wave-Driven Wind Jets in the Marine Atmospheric
403 Boundary Layer, *J. Atmos. Sci.*, 65(8), 2646-2660, doi.org/10.1175/2007JAS2562.1, 2008.
- 404 Jarosz, E., Mitchell, D. A., Wang, D. W., and Teague, W. J.: Bottom-up determination of air-
405 sea momentum exchange under a major tropical cyclone, *Science*, 315, 1707-1709, 2007.
- 406 Jones, I. S. F., and Toba, Y.: Wind stress over the ocean. Cambridge University Press, New
407 York, 2001.
- 408 Kalnay, E., Kanamitsu, M., Kistler, R., Collins, W., Daeven, D., Gandin, L., Iredell, M., Saha,
409 S., White, G., Woollen, J., Zhu, Y., Chelliah, M., Ebisuzaki, W., Higgins, W., Janowiak, J.,
410 Mo, K. C., Ropelewski, C., Wang, J., Leetmaa, A., Reynolds, R., Jenne, R., and Joseph, D.:
411 The NCEP/NCAR 40-year reanalysis project, *Bull. Amer. Meteor. Soc.*, 77(3), 437-471,
412 1996.
- 413 Kukulka, T., Hara, T., and Belcher, S. E.: A model of the air-sea momentum flux and
414 breaking-wave distribution for strongly forced wind waves, *J. Phys. Oceanogr.*, 37(7),
415 1811-1828, doi:10.1175/JPO3084.1, 2007.
- 416 Large, W. G., and Pond, S.: Open ocean momentum flux measurements in moderate to strong
417 winds, *J. Phys. Oceanogr.*, 11(3), 324-336, doi:10.1174/1520-
418 0485(1981)011<0324:OOMFMI>2.0.CO;2, 1981.
- 419 Large, W. G., and Yeager, S. G.: Diurnal to decadal global forcing for ocean and sea-ice
420 models: the data sets and flux climatologies, Technical Note NCAR/TN-460+STR, NCAR,
421 Boulder, CO, 2004.
- 422 Lüpkes, C., Gryanik, V. M., Hartmann, J., and Andreas, E. L.: A parameterization, based on
423 sea-ice morphology, of the neutral atmospheric drag coefficients for weather prediction and
424 climate models, *J. Geophys. Res.: Atmospheres*, 117(D13), doi:10.1029/2012JD01763,
425 2012.
- 426 Peng, S., and Li, Y.: A parabolic model of drag coefficient for storm surge simulation in the
427 South China Sea, *Sci. Rep.*, 5(15496), doi:10.1038/srep15496, 2015.



- 428 Rieder, K. F., Smith, J. K., and Weller, R. A.: Observed directional characteristics of the wind,
429 wind stress, and surface waves on the open ocean, *J. Geophys. Res.: Oceans.*, **99**(C11),
430 589-596, doi:10.1029/94JC02215, 1994.
- 431 Sahlée, E., Drennan, W. M., Potter, H. , and Rebozo, M. A.: Waves and air-sea fluxes from a
432 drifting asis buoy during the southern ocean gas exchange experiment, *J. Geophys. Res.:*
433 *Oceans*, **117**(C08003), doi: 10.1029/2012JC008032, 2012.
- 434 Shutler, J. D., Piolle, J-F., Land, P. E., Woolf, D. K., Goddijn-Murphy, L., Paul, F., Girard-
435 Arduin, F., Chapron, B., and Donlon, C. J.: FluxEngine: a flexible processing system for
436 calculating air-sea carbon dioxide gas fluxes and climatologies, *J. Atmos. Oceanic*
437 *Technol.*, **33**(4), 741-756, doi:10.1175/JTECH-D-14-00204.1, 2016.
- 438 Taylor, G. I.: Skin friction of the wind on the Earth's surface, *Proc. Roy. Soc. London*, A92,
439 196-199, 1916.
- 440 Trenberth, K. E., Large, W. G., and Olson, J. G.: The effective drag coefficient for evaluating
441 wind stress over the Oceans, *J. Climate*, **2**(12), 1507-1516, doi:10.1175/1520-
442 0422(1989)002<1507:TEDCFE>2.0.CO;2, 1989.
- 443 Wu, J.: Wind stress and surface roughness at air-sea interface, *J. Geophys. Res.*, 74(2), 444-
444 455, doi:10.1029/JB074i002p00444, 1969.
- 445 Wu, J.: Wind stress coefficients over the sea surface near neutral conditions – A revisit, *J.*
446 *Phys. Oceanogr.*, **10**(5), 727-740, doi:10.1175/1520-
447 0485(1980)010<0727:WSCOSS>2.0.CO;2, 1980.
- 448 Wu, J.: Wind-stress coefficients over sea surface from breeze to hurricane, *J. Geophys. Res.*,
449 **87**(C12), 9704-9706, doi: 10.1029/JC087iC12p09704, 1982.
- 450 Zilitinkiewicz, S. S., Monin, A. S., and Czalikow, S. W.: Dynamika Morza. Wzajemne
451 oddziaływanie morza i atmosfery, *Studia i materiały oceanologiczne*, vol. 22. Poland, 1978.
- 452 Yelland, M., and Taylor, P. K.: Wind stress measurements from the open ocean, *J. Phys.*
453 *Oceanogr.*, **26**(4), 541-558, doi:10.1175/1520-0485(1996)026<0541:WSMFTO>2.0.CO;2,
454 1966.
- 455
456
457
458
459
460
461
462
463
464
465
466
467
468
469
470



471 **Table 1.** Average annual mean values of momentum flux (wind stress) [N m^{-2}] for all the
472 studied regions and parameterizations. In each column the percentage values are normalized
473 to A12, the parameterization that produced the smallest average flux values.

474

475 **Figure 1.** The drag coefficient parameterization used in the study (Eqs. 8-14) as a function of
476 wind speed U_{10} (m s^{-1}).

477

478 **Figure 2.** Maps of momentum flux [N m^{-2}] across the sea surface (wind stress) for boreal
479 winters ((**a**) and (**c**)) and summers ((**b**) and (**d**)) for Wu (1969) and A12 drag coefficient
480 parameterizations (the two parameterizations with the highest and lowest average values,
481 respectively).

482

483 **Figure 3.** Monthly average momentum flux values [N m^{-2}] for (**a**) global ocean, (**b**) North
484 Atlantic, (**c**) European Arctic, and (**d**) tropical ocean. The regions are defined in the text.

485

486 **Figure 4.** The drag coefficient values for Large and Yeager (2004) and Andreas et al., (2012)
487 parameterization as a function of wind speed U_{10} (m s^{-1}).

488

489 **Figure 5.** Annual average momentum flux values for (**a**) European Arctic and (**b**) Tropical
490 ocean. The vertical solid line is the average of all seven parameterization and the dashed lines
491 are standard deviations for the presented values. Global and the North Atlantic results are not
492 shown because the relative values for different parameterizations are very similar (see Table
493 1), scaling almost identically between the basins.

494

495 **Figure 6.** Annual mean wind speed U_{10} (m s^{-1}) in the study area—the North Atlantic and the
496 European Arctic (north of the red line).

497

498



499 **Table 1.** Average annual mean values of momentum flux (wind stress) [N m^{-2}] for all the
 500 studied regions and parameterizations. In each column the percentage values are normalized
 501 to A12, the parameterization that produced the smallest average flux values.
 502

	Global	North Atlantic	Arctic	W. Spitsbergen	Tropics
Wu (1969)	0.322 (114 %)	0.330 (114 %)	0.375 (114 %)	0.360 (114 %)	0.261 (119 %)
Garratt (1977)	0.307 (109 %)	0.316 (109 %)	0.358 (109 %)	0.344 (110 %)	0.251 (115 %)
Wu (1982)	0.311 (110 %)	0.320 (110 %)	0.363 (110 %)	0.349 (111 %)	0.255 (117 %)
NCEP/NCAR	0.303 (107 %)	0.312 (107 %)	0.353 (107 %)	0.341 (108 %)	0.258 (118 %)
Yelland & Taylor (1996)	0.297 (105 %)	0.306 (105 %)	0.348 (106 %)	0.335 (107 %)	0.245 (112 %)
Large & Yeager (2004)	0.285 (101 %)	0.293 (101 %)	0.333 (101 %)	0.320 (102 %)	0.236 (108 %)
Andreas et al., (2012)	0.283 (100 %)	0.290 (100 %)	0.329 (100 %)	0.314 (100 %)	0.219 (100 %)

503
504

505

506

507

508

509

510

511

512

513

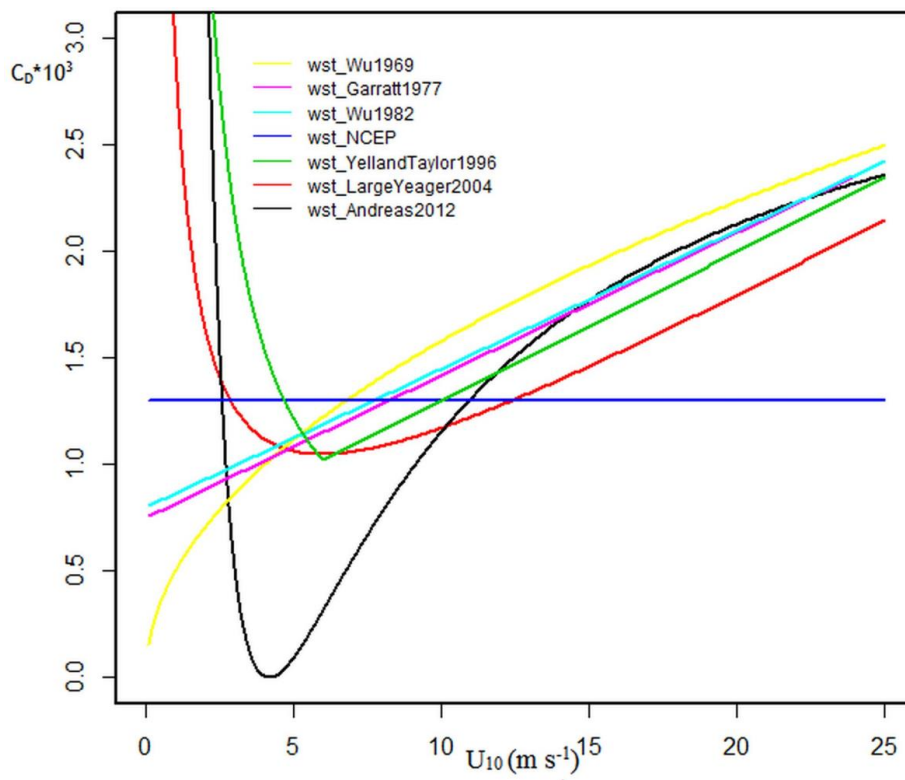
514

515

516



517 **Figure 1.** The drag coefficient parameterization used in the study (Eqs. 8-14) as a function of
518 wind speed U_{10} (m s^{-1}).



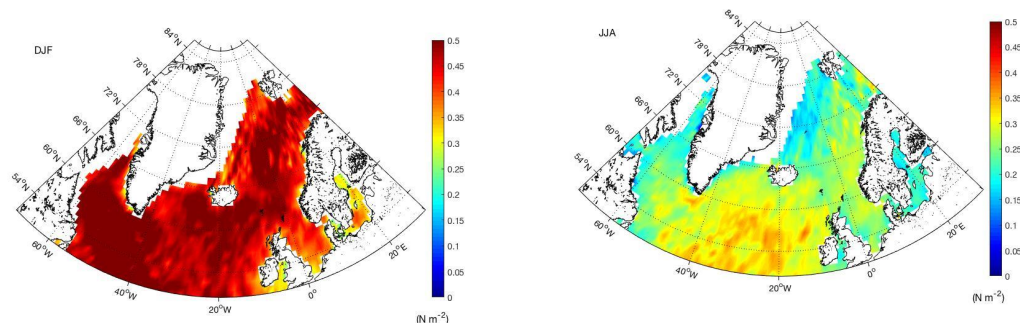
519
520
521
522
523
524
525
526
527
528



529 **Figure 2.** Maps of momentum flux [N m^{-2}] across the sea surface (wind stress) for boreal
530 winters ((a) and (c)) and summers ((b) and (d)) for Wu (1969) and A12 drag coefficient
531 parameterizations (the two parameterizations with the highest and lowest average values,
532 respectively).
533

534 (a) Wu, (1969)

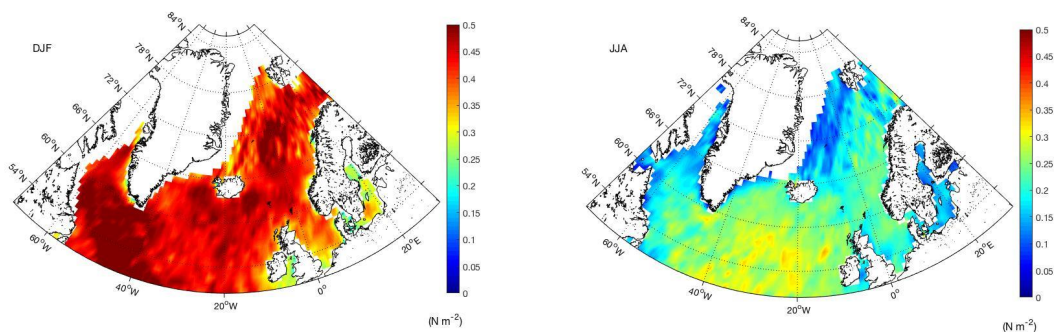
(b) Wu (1969)



536 (c) Andreas, et al., (2012)

(d) Andreas, et al., (2012)

537



538

539

540

541

542

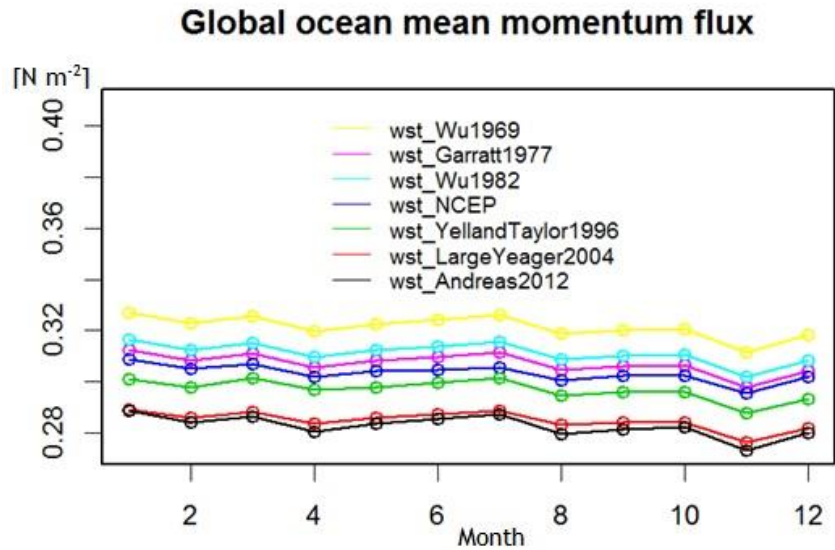
543

544

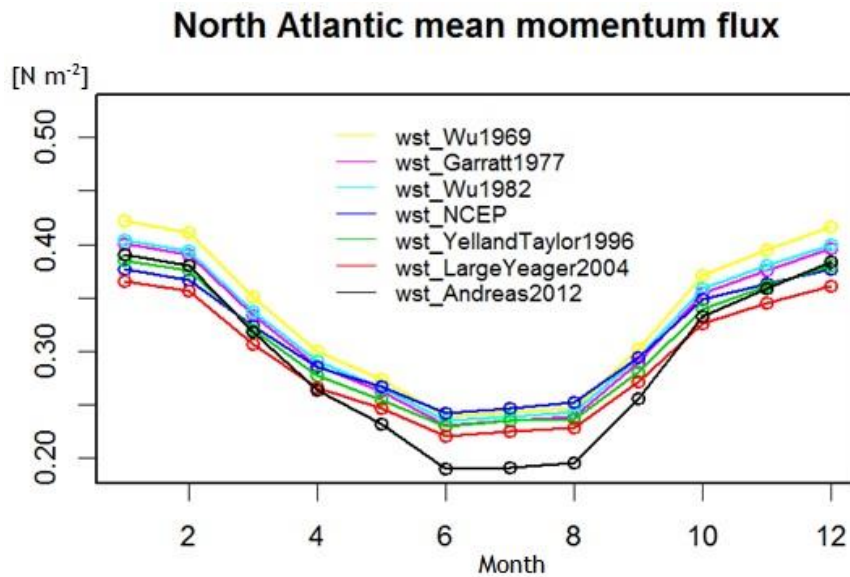


545 **Figure 3.** Monthly average momentum flux values [N m^{-2}] for (a) global ocean, (b) North
546 Atlantic, (c) European Arctic, and (d) Tropical ocean. The regions are defined in the text.
547 (a)

548



568
569 (b)



570
571
572
573



574 (c)

575

576

577

578

579

580

581

582

583

584

585 (d)

586

587

588

589

590

591

592

593

594

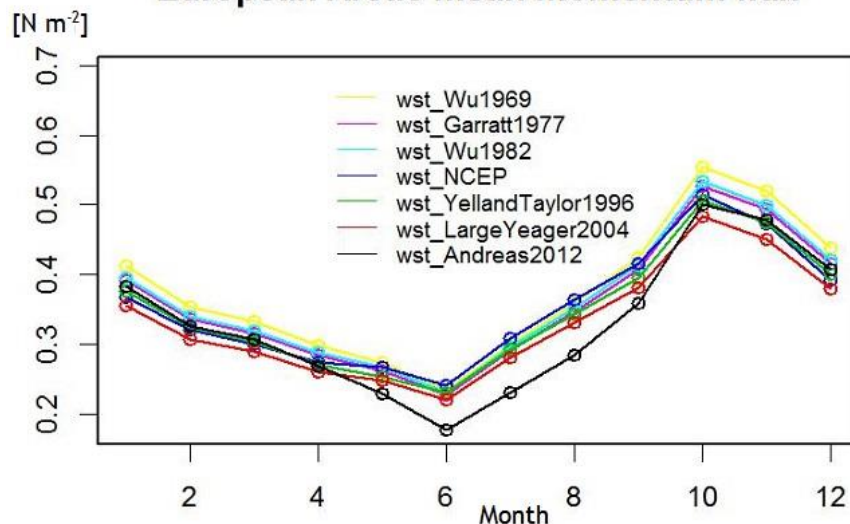
595

596

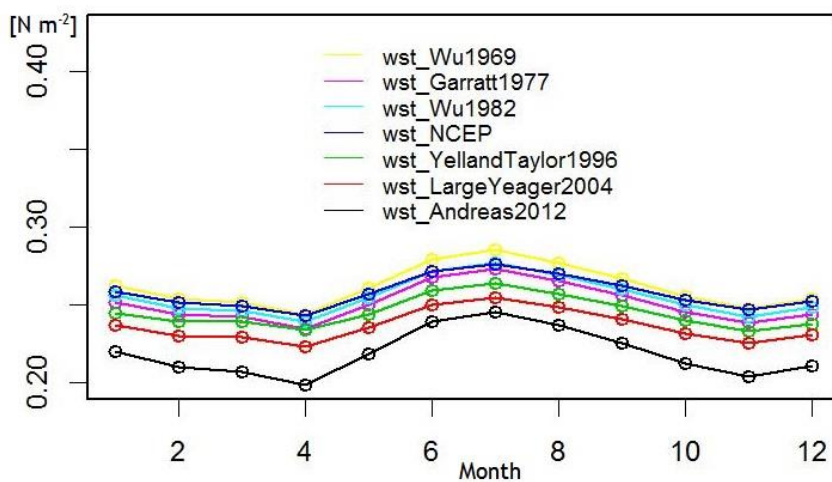
597

598

European Arctic mean momentum flux

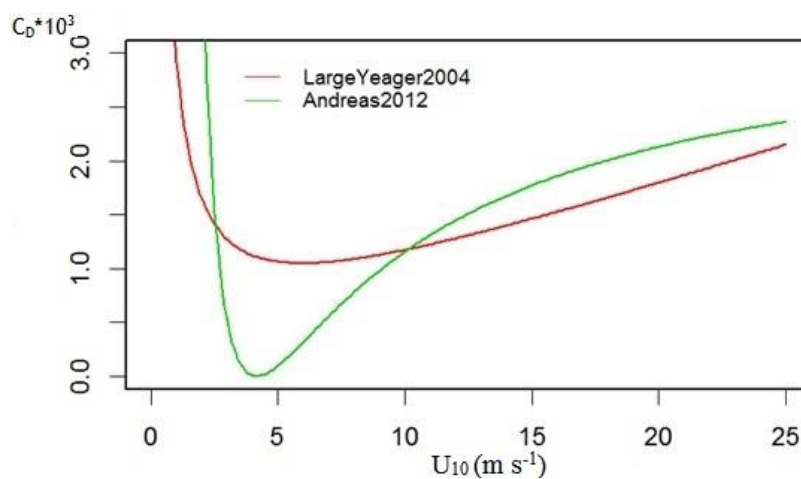


Tropical Ocean mean momentum flux





599 **Figure 4.** The drag coefficient values for Large and Yeager (2004) and Andreas et al., (2012)
600 parameterization as a function of wind speed U_{10} (m s^{-1}).
601



602

603

604

605

606

607

608

609

610

611

612

613

614

615

616

617

618

619

620

621

622

623

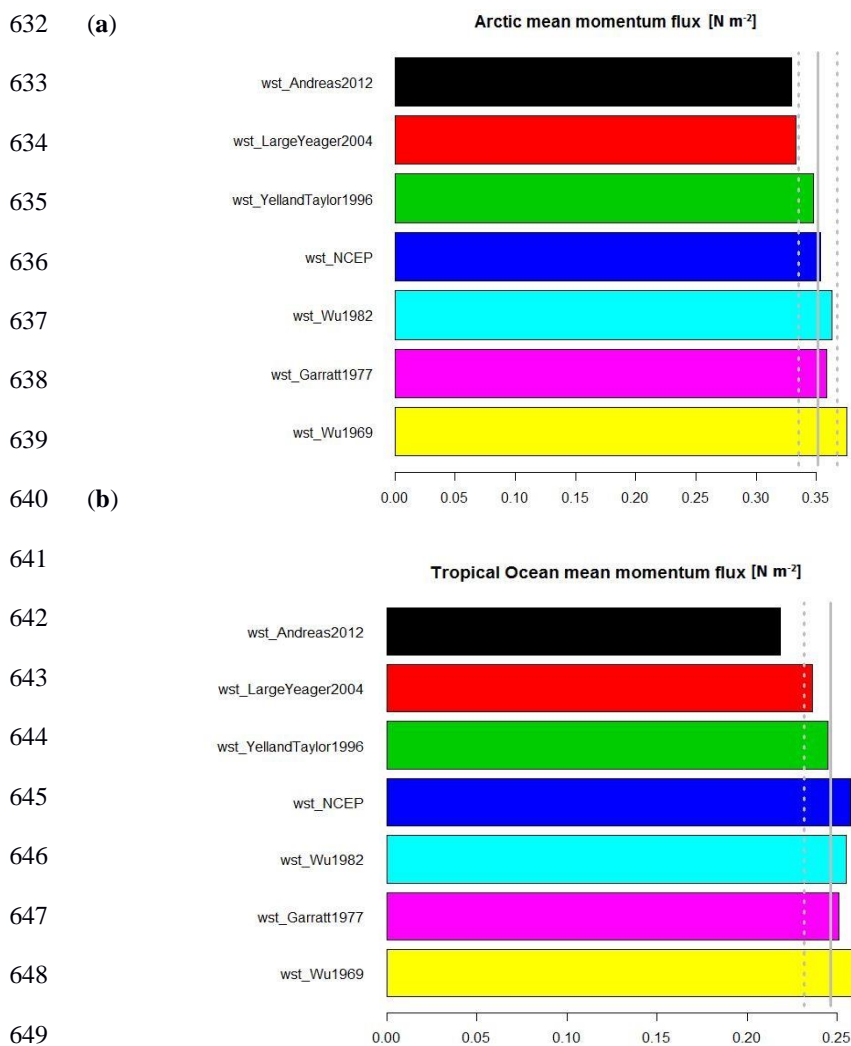
624

625

626



627 **Figure 5.** Annual average momentum flux values for (a) European Arctic and (b) Tropical
628 ocean. The vertical solid line is the average of all seven parameterization and the dashed lines
629 are standard deviations for the presented values. Global and the North Atlantic results are not
630 shown because the relative values for different parameterizations are very similar (see Table
631 1), scaling almost identically between the basins.



650
651
652
653
654



655 **Figure 6.** Annual mean wind speed U_{10} (m s^{-1}) in the study area—the North Atlantic and the
656 European Arctic (north of the red line).
657
658

